Role of phosphatidylinositol 3′-kinase/AKT pathway in diffuse large B-cell lymphoma survival

Shahab Uddin, Azhar R. Hussain, Abdul K. Siraj, Pulicat S. Manogaran, Naif A. Al-Jomah, Azadali Moorji, Valerie Atizado, Fouad Al-Dayel, Asim Belgaumi, Hassan El-Solh, Adnan Ezzat, Prashant Bavi, and Khawla S. Al-Kuraya

Phosphatidylinositol 3′-kinase (PI3K) is a key player in cell-growth signaling in a number of lymphoid malignancies, but its role in diffuse large B-cell lymphoma (DLBCL) has not been fully elucidated. Therefore, we investigated the role of the PI3K/AKT pathway in a panel of 5 DLBCL cell lines and 100 clinical samples. Inhibition of PI3K by a specific inhibitor, LY294002, induced apoptosis in SUDHL4, SUDHL5, and SUDHL10 (LY-sensitive) cells, whereas SUDHL8 and OCI-LY19 (LY-resistant) cells were refractory to LY294002-induced apoptosis. AKT was phosphorylated in 5 of 5 DLBCL cell lines and inhibition of PI3K caused dephosphorylation/inactivation of constitutively active AKT, FOXO transcription factor, and GSK3 in LY-sensitive cell lines. In addition, there was a decrease in the expression level of inhibitory apoptotic protein, XIAP, in the DLBCL cell lines sensitive to LY294002 after treatment. However, no effect was observed in XIAP protein levels in the resistant DLBCL cell lines following LY294002 treatment. Finally, using immunohistochemistry, p-AKT was detected in 52% of DLBCL tumors tested. Furthermore, in univariate analysis, high p-AKT expression was associated with short survival. In multivariate analysis, this correlation was no longer significant. Altogether, these results suggest that the PI3K/AKT pathway may be a potential target for therapeutic intervention in DLBCL. (Blood. 2006;108: 4178-4186)

Introduction

B-cell lymphoma represents the malignant counterpart of normal B cells arrested at specific maturational stages. Diffuse large B-cell lymphoma (DLBCL) is considered to be the most common type of lymphoma in adults, accounting for 30% to 40% of cases of non-Hodgkin lymphoma.[1] Although patients with DLBCLs are potentially curable with combination chemotherapy, the disease proves fatal in approximately 50% of patients.[2] The cause of most DLBCLs remains unknown; however, dysregulation of apoptosis or defective repair plays a role in lymphogenesis.[3]

A number of constitutively activated growth signaling pathways have frequently been observed in DLBCL including protein kinase AKT and nuclear factor κB (NF-κB) transcription factor.[4-6] Protein kinases have been implicated as having crucial roles in regulating cell growth, metabolic responses, cell proliferation, migration, and apoptosis, which altogether contribute to tumorigenesis. Constitutive activation of these protein kinases, mainly by phosphorylation, has been implicated as contributing to malignant phenotypes in a number of human cancers.[7-9] AKT is a serine threonine kinase that gets activated on growth factor and cytokine stimulation. When phosphoinositide-3,4,5-triphosphate (PIP_3) is generated by phosphatidylinositol 3′-kinase (PI3K) in response to an intracellular signal, it binds to the PH domain of AKT and translocates to the plasma membrane resulting in the activation of phosphoinositide-dependent protein kinases (PDK1 and PDK2). Activated PDK1 and PDK2 phosphorylate at the Thr308 and Ser473 residues of the AKT kinase domain, resulting in its activation.[10] AKT protein kinase regulates a variety of cellular processes, including apoptosis, cell survival, and proliferation.[11-13] AKT-mediated phosphorylation may alter the activity of proteins such as caspase-9, some Bcl-2 family members, and NF-κB and other transcription factors that trigger or restrain apoptosis. PI3K/Akt deregulation may also contribute to tumorigenesis, metastasis, and resistance to chemotherapy.[14,15] For this reason, the PI3K/Akt signaling pathway might represent a promising target for therapeutic intervention. Actually, the PI3K inhibitors LY294002 and wortmannin were observed to exert antitumor activity in animal cell models.[14,15] AKT has been shown to play critical role in the tumorigenesis of many cell types.[16-19] The biologic significance of AKT kinase activity in lymphogenesis has been recently established in a mouse model.[20]

A number of studies have shown that the cell-death–inducing effect of chemotherapy depends on induction of apoptosis and that disruption of the apoptosis signaling cascade may thus be an important cause for chemotherapy resistance.[21,22] Two major apoptosis pathways have been described[23,24]: (1) an intrinsic mitochondrial, stress-induced pathway involving mitochondrial signaling and caspases and (2) an extrinsic, death receptor–mediated pathway. The stress-induced pathway can be inhibited at many levels. The most potent inhibitors of this pathway appear to be Bcl-2 and the X-linked inhibitor of apoptosis (XIAP).[25,26]

To explore the role of PI3K in the survival, proliferation, and apoptosis of DLBCL, we used a panel of DLBCL cell lines to examine the involvement of AKT and its substrates, forkhead transcription factors, and GSK3 in these cells. We next examined whether inhibition of PI3K plays any role in the regulation of proapoptotic and antiapoptotic members of the Bcl-2 family in materializing the induction of apoptosis and cell growth inhibition.

From the Research Center, King Fahad National Center for Children's Cancer and Research, Biological and Medical Research, Department of Pathology, Pediatric Hematology-Oncology, King Faisal Cancer Center, King Faisal Specialist Hospital and Research Center, Riyadh, Saudi Arabia.

Submitted April 12, 2006; accepted July 24, 2006. Prepublished online as *Blood* First Edition Paper, 8/31/2006; DOI 10.1182/blood-2006-04-016907.

The online version of this article contains a data supplement.

The publication costs of this article were defrayed in part by page charge payment. Therefore, and solely to indicate this fact, this article is hereby marked "advertisement" in accordance with 18 USC section 1734.

We further analyzed the role of inhibition of PI3K on the mitochondrial-mediated apoptotic pathway in DLBCL cells via the release of cytochrome *c* into cytosol. Finally, we studied the release of cytochrome *c*–propagating death signals to caspase-3, causing its activation and leading to the cleavage of PARP and eventually cell death after PI3K inhibition. To study the clinical relevance of the PI3K/AKT pathway in DLBCL, p-AKT expression was studied in a group of 100 patients using tissue microarray technology. Our data show that overexpression of p-AKT in DLBCL is associated with poor outcome.

Patients, materials, and methods

Materials and methods

Cell culture. The human DLBCL cell lines SUDHL4, SUDHL5, SUDHL8, SUDHL10, and OCI-LY19 were obtained from Deutsche Sammlung von Mikroorganismen und Zellkulturen (DSMZ, Braunschweig, Germany). The cell lines were cultured in RPMI 1640 medium supplemented with 20% (vol/vol) fetal bovine serum (FBS), 100 U/mL penicillin, and 100 U/mL streptomycin at 37°C in a humidified atmosphere containing 5% CO_2. All the experiments were performed in RPMI 1640 containing 5% serum.

PI3K/AKT inhibitors. LY294002 and AKT inhibitor (1L-6-hydroxymethyl-chiro-inositol 2-(R)-2-O-methyl-3-O-octadecylcarbonate) were obtained from Calbiochem (San Diego, CA). Wortmannin was obtained from Sigma Chemical (St Louis, MO).

Reagents and antibodies. Anti–cytochrome *c*, anti–caspase-3, and anti-PARP antibodies were purchased from Santa Cruz Biotechnology (Santa Cruz, CA). The anti–phospho-AKT (Ser473), phospho-AKT (Ser473) blocking peptide, anti–phospho-GSK3α/β, anti–phospho-FKHRL1, anti–cleaved caspase-3, and anti-BID antibodies were purchased from Cell Signaling Technologies (Beverly, MA). Anti–β-actin was purchased from Abcam (Cambridge, United Kingdom). Anti–caspase-8 antibody was obtained from R&D Systems (Minneapolis, MN). Antibody against Ki-67 was purchased from Dako (Carpinteria, CA). The TdT-mediated dUTP nick-end labeling (TUNEL) assay kit was obtained from MBL (Watertown, MA). Annexin V was purchased from Molecular Probes (Eugene, OR). The apoptotic DNA ladder kit was obtained from Roche (Penzberg, Germany).

Cell death assay

Following indicated treatments, cells were incubated with trypan blue for 5 to 10 minutes at room temperature. Trypan blue–positive and total cells were counted per microscope field for a total of 4 fields per condition. The proportion of cell death was calculated by dividing the number of dead cells by total number/field.

TUNEL assay

DLBCL cell lines were treated with LY294002 as described in the figure legends. Apoptotic cells were measured using the TUNEL assay as described earlier.[27] Briefly, after 24 hours of treatment with different concentrations of LY294002, 1×10^6 cells were washed twice with PBS containing 0.2% BSA and fixed with 4% paraformaldehyde at 4°C for 30 minutes. This was followed by 2 washes with PBS containing 0.2% BSA and the cells were permeabilized in 70% ethanol at −20°C for 30 minutes. The cells were then washed twice with PBS containing 0.2% BSA and incubated with 30 μL TdT buffer (TdT buffer II, FITC-dUTP, and TdT in the ratio of 18:1:1) for 1 hour at 37°C. This was followed by 2 washes with PBS and the cells were resuspended in 500 μL PBS. Stained cells were analyzed using FACScan flow cytometry equipped with a Cell Quest data analysis program (Becton Dickinson, San Diego, CA).

Annexin V staining

DLBCL cell lines were treated with different concentrations of LY294002 and AKT inhibitor (1L-6-hydroxymethyl-chiro-inositol 2-(R)-2-O-methyl-3-O-octadecylcarbonate) as described in the figure legends. Cells were harvested and the percentage apoptosis was measured by flow cytometry after staining with fluorescein-conjugated annexin V and propidium iodide (PI; Molecular Probes) as described previously.[28,29] We scored viable cells as those that are negative for annexin V and PI. Percentage of apoptosis was calculated from the reduction of the number of viable cells between the treated and untreated samples. The amount of necrotic cells (annexin V^-, PI^+) was always minimal.

Cell cycle analysis

Cell lines were treated either with or without LY294002 for 24 hours and the cells were washed once with PBS, resuspended in 500 μL hypotonic staining buffer (sodium citrate 250 mg, Triton X 0.75 mL, PI 25 μg, ribonuclease A 5 μg, and 250 mL water), and analyzed by flow cytometry as described previously.[30]

DNA laddering

Cells (2×10^6) were treated with and without 25 μM LY294002 for 24 hours. The cells were then harvested and resuspended in 200 μL 1 × PBS. Then 200 μL lysis buffer containing 6 M guanidine HCl, 10 mM urea, 10 mM Tris-HCl, and 20% Triton X (vol/vol), pH 4.4, was added to the cells and incubated for 10 minutes at room temperature. Isopropanol (100 μL) was added and shaken for 30 seconds on a vortex. Then samples were passed through a filter and spun at 4500 *g* for 1 minute and the supernatant was discarded. The pellets were washed 3 times with wash buffer containing 20 mM NaCl, 2 mM Tris-HCl, and 80% ethanol. The pellets were then transferred into a new 1.5-mL tube and eluted with 200 μL prewarmed elution buffer. After measuring the DNA, 2 μg DNA was electrophoresed on a 1.5% agarose gel containing ethidium bromide at 75 V for 2 hours and visualized using a UV light source.

Cell lysis and immunoblotting

Cells were treated with LY294002 as described in the figure legends and lysed as previously described.[31,32] Briefly, cell pellets were resuspended in phosphorylation lysis buffer (0.5-1.0% Triton X-100, 150 mM NaCl, 1 mM EDTA, 200 μM sodium orthovanadate, 10 mM sodium pyrophosphate, 100 mM sodium fluoride, 1.5 mM magnesium chloride, 1 mM phenylmethyl sulfonyl fluoride, 10 μg/mL aprotinin). Protein concentrations were assessed by Bradford assay before loading the samples. Equal amounts of proteins were separated by sodium dodecyl sulfate-polyacrylamide gel electrophoresis (SDS-PAGE) and transferred to polyvinylidene diflouride membranes (Immobilon, Millipore). Immunoblotting was performed with different antibodies and visualized by an enhanced chemiluminescence (ECL; Amersham, Arlington Heights, IL) method.

Assay for cytochrome *c* release

Release of cytochrome *c* from mitochondria was assayed as described earlier.[33] Briefly, cells were treated with and without LY294002 as described in figure legends and centrifuged at 1000*g*. Cell pellets were resuspended in 5 volumes of a hypotonic buffer (20 mM HEPES-KOH, pH 7.5, 10 mM KCl, 1.5 mM $MgCl_2$, 1 mM EDTA, 1 mM EGTA, 1 mM DTT, 20 μg/mL leupeptin, 10 μg/mL aprotinin, 250 mM sucrose) and incubated for 15 minutes on ice. Cells were homogenized by 15 to 20 passages through a 22-gauge needle, 1.5 inches long. The lysates were centrifuged at 1000*g* for 5 minutes at 4°C to pellet nuclei and unbroken cells. Supernatants were collected and centrifuged at 12 000*g* for 15 minutes. The resulting mitochondrial pellets were resuspended in lysis buffer. Supernatants were transferred to new tubes and centrifuged again at 12 000*g* for 15 minutes and resulting supernatants representing cytosolic fractions were separated. Twenty to 25 μg protein from the cytosolic and mitochondrial fraction of each sample was analyzed by immunoblotting using an anti–cytochrome *c* antibody.

Measurement of mitochondrial potential using the JC-1 assay kit

Cells (1×10^6) cells were treated with 25 μM LY294002 for 24 hours. Cells were washed twice with PBS and suspended in mitochondrial incubation buffer. JC-1 (5, 5′, 6, 6′-tetrachloro-1, 1′, 3,3′-tetraethylbenzimidazolylcarbocyanine iodide) was added to a final concentration of 10 μM and cells were incubated at 37°C in the dark for 30 minutes. Cells were washed twice with PBS and resuspended in 500 μL mitochondrial incubation buffer and mitochondrial membrane potential (percent of green and red aggregates) was determined by flow cytometry as described previously.[34]

Patient selection and tissue microarray construction

One hundred patients with DLBCL diagnosed between 1994 and 2004 were selected from the files of the King Faisal Specialist Hospital and Research Centre. All samples were analyzed in a tissue microarray (TMA) format. TMA construction was performed as described earlier.[35] Briefly, tissue cylinders with a diameter of 0.6 mm were punched from representative tumor regions of each donor tissue block and brought into recipient paraffin block using a homemade semiautomatic robotic precision instrument. An overview of a DLBCL TMA section is shown in Figure 6A. Three 0.6-mm cores of DLBCL were arrayed from each case.

Patients were reclassified according to the World Health Organization (WHO) classification.[36] Age, tumor stage, lactate dehydrogenase (LDH) level, performance status, and the number of extranodal sites of the disease were used to determine the International Prognostic Index (IPI).[37] For statistical analysis, patients were classified as low risk, low-intermediate risk, high-intermediate risk, and high risk. The number of risk categories was condensed from 4 to 2 as follows: a low-risk group encompassing patients defined in the IPI as low and low-intermediate risk and a high-risk group encompassing patients defined in the IPI as high-intermediate and high risk. The Institutional Review Board of the King Faisal Specialist Hospital & Research Centre approved the study, in accordance with the Declaration of Helsinki.

Immunohistochemistry

Tissue microarray sections (3-4 μm thick) were stained with the p-AKT (Ser473) antibody using Survival Marker: Signal Stain Phospho-AKT (Ser473) immunohistochemistry (IHC) detection kit (Cell Signaling Technology, product no. 8100). The IHC protocol mentioned in the kit was followed using all the reagents provided in the kit. Antigen retrieval was performed by heating the slides for 10 minutes at 96°C in citrate buffer. Incubating the tissue in blocking solution blocked nonspecific binding. Endogenous peroxidase activity was quenched using peroxidase quench supplied along with the kit. Endogenous biotin was blocked and counterstaining was carried out with Harris hematoxylin.

Only fresh-cut slides were stained simultaneously to minimize the influence of slide aging and maximize repeatability and reproducibility of the experiment. Two types of negative controls were used. One was the negative control in the kit in which the primary antibody was omitted. A preabsorption experiment using p-AKT Ser473 blocking peptide (Cell Signaling Technology, product no. 1140) was used as the second negative control.

p-AKT was scored depending on an intensity scale ranging from 0 to 2. Scoring was performed as follows: 0, no appreciable staining in tumor cells; 1, barely detectable staining in tumor cells similar to p-AKT expression in the B-cell areas of normal lymphoid tissues; 2, readily appreciable staining distinctly marking tumor cell ranging from moderate to intense. This scoring system has been reported previously.[38,39] For statistical analysis, all cases with score 0 to 1 were grouped as p-AKT$^-$ and cases with score 2 were grouped as p-AKT$^+$. The DLBCL cases were arrayed in 3 replica blocks and IHC scoring of p-AKT was performed on all blocks. The p-AKT expression was recorded in all 3 cores and the core showing maximal staining was taken as the final score, as reported previously.[40]

Slides of normal lymphoid tissue (4 tonsils and 1 lymph node) were stained with p-AKT antibody simultaneously in the same IHC run with DLBCL array slides to study the p-AKT expression in the B-cell areas of these normal lymphoid tissues. The staining for p-AKT in the B-cell areas of these normal tissues ranged from complete absence of staining to weak staining. This was scored as 0 or 1. Moderate to high staining was scored as 2. All the normal lymphoid tissues showed a p-AKT expression ranging between 0 and 1. The slides were all evaluated in 1 day by one pathologist (P.B.) to minimize interobserver and intraobserver variability of the results.

Statistics

The software used for statistical analysis was Statview 5.0 (SAS Institute, Cary, NC). For survival analysis, patients with p-AKT weakly positive (score 1) and negative (score 0) tumors were grouped together to emphasize on p-AKT–overexpressing tumors. Survival curves were constructed according to the Kaplan-Meier method. Differences between the curves were analyzed using the log-rank test. The limit of significance for all analyses was defined as a P value of .05; 2-sided tests were used in all calculations.

Results

Inhibition of PI3K/AKT induces apoptosis in DLBCL cells

The PI3K pathway has been implicated in the growth and survival of a range of cell types,[41] but its effects on DLBCL cells have not been analyzed in detail. We sought to determine whether the inhibition of PI3K by its specific inhibitor, LY294002, caused cell death and apoptosis in DLBCL cells. LY294002 is a synthetic flavanoid that acts as a potent, competitive, reversible inhibitor of the ATP-binding site of class I PI3K.[42] We first sought to determine the dose-dependent effect of LY294002 on the viability of DLBCL cell lines. SUDHL4, SUDHL8, and OCI-LY19 cells were treated with various doses ranging from 5 to 100 μM LY294002 for 24 hours and cell death was determined by trypan blue exclusion assay. As shown in Figure 1A, LY294002 treatment caused cell death in a dose-dependent manner in the SUDHL4 cell line with an IC_{50} of about 12 μM. On the other hand, SUDHL8 and OCI-LY19 required higher doses of LY294002 to induce cell death (IC_{50} = 80-90 μM). Because the possibility of nonspecific and toxic effects at higher doses cannot be ruled out, we chose a working concentration of 10 to 25 μM, which has previously been shown to be specific for inhibition of PI3K.[43] We further sought to determine the effect of LY294002 on cell death in all DLBCL cell lines. LY294002 treatment caused a significant ($P < .001$) loss of viability at 10 and 25 μ M in SUDHL4, SUDHL5, and SUDHL10 cell lines, whereas SUDHL8 and OCI-LY19 were refractory to LY294002-induced cell death (Figure 1B).

To determine whether cell death induced by PI3K inhibition growth was attributable to cell-cycle arrest or apoptosis, DLBCL cells were treated with and without 10 and 25 μM LY294002 for 24 hours. Cell-cycle fractions were determined by flow cytometry. As shown in Figure 1C, the sub-G_1 population of SUDHL4 cells was increased from 4.96% in the control to 28.07% and 70.60% at 10 and 25 μM LY294002, respectively. Similar results were obtained in SUDHL5, from 2.42% to 23.54 and 42.20%, and SUDHL10, from 4.54% to 21.01% and 76.12% increase in the sub-G_1 population. This increase in sub-G_1 populations was accompanied by loss of cells in G_0/G_1, S and G_2/M phases. On the other hand, SUDHL8 and OCI-LY19 cell lines did not show appreciable apoptotic sub-G_1 population fractions after LY294002 treatment. To evaluate the possibility that early cell-cycle arrest may be occurring prior to the initiation of apoptosis, SUDHL4 and SUDHL5 cell lines were treated with 25 μM LY294002 for various time periods and cell-cycle status was evaluated by flow cytometry. LY294002

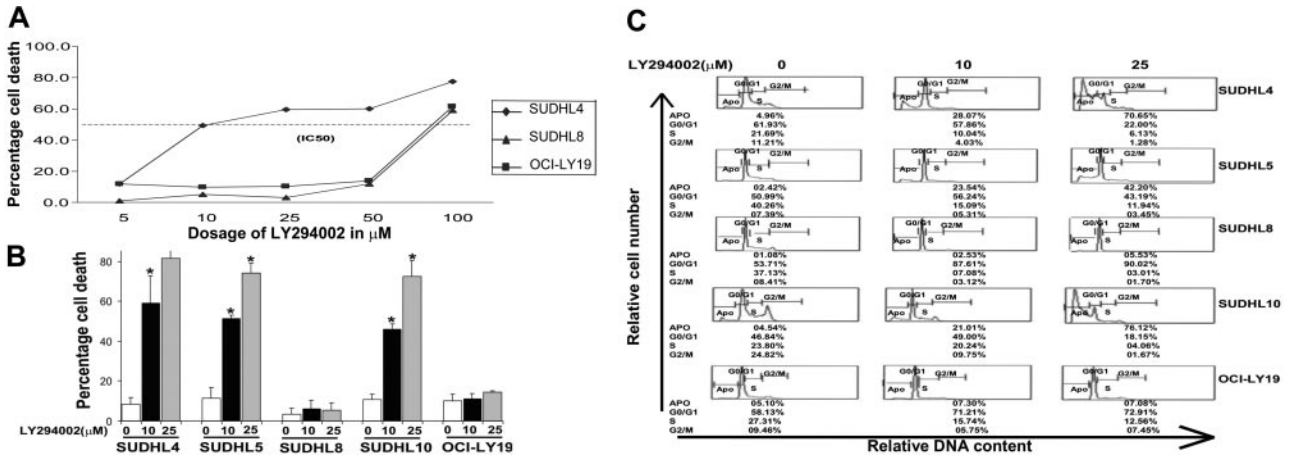

Figure 1. Effect of LY294002 treatment on cell death in DLBCL cell lines. (A) Dose-response curves to compare IC_{50} of LY294002 in DLBCL cell lines. SUDHL4, SUDHL8, and OCI-LY19 cells were treated with various doses (5-100 μM) of LY294002 for 24 hours. Cell death was measured and IC_{50} was determined by trypan blue exclusion assay as described in "Patients, materials, and methods." (B) LY294002 inhibits cell viability in DLBCL cell lines. SUDHL-4, SUDHL-5, SUDHL-8, SUDHL-10, and OCI-LY19 cells were treated with 10 and 25 μM LY294002 for 24 hours. Percentage cell death was scored using trypan blue exclusion dye. The graph displays the mean ± SD of 3 independent experiments. *$P < .001$, statistically significant (Student *t* test). (C). LY294002 treatment increases sub-G_1 (Apo) population in DLBCL cells. SUDHL-4, SUDHL-5, SUDHL-8, SUDHL-10, and OCI-LY19 cells were treated with 10 and 25 μM LY294002 for 24 hours. Thereafter, the cells were washed, stained with propidium iodide, and analyzed for DNA content by flow cytometry as described in "Patients, materials, and methods."

treatment caused apoptosis in a time-dependent manner without arresting cells in G_0/G_1 phase at any time point, suggesting that there is no cell-cycle arrest (Figure S1, available on the *Blood* website; see the Supplemental Materials link at the top of the online article). It has been reported that cells with these features are those dying of apoptosis.[44] These results indicate that DLBCL cells underwent apoptosis rather than cell-cycle arrest following LY294002 treatment.

To further confirm that this increase in the sub-G_1 population is indeed apoptosis, DLBCL cells were treated with 10 and 25 μM LY294002 and apoptotic cells were assayed by annexin V/PI dual staining. As shown in Figure 2A, treatment with LY294002 of SUDHL4, SUDHL5, and SUDHL10 cells resulted in apoptosis, whereas SUDHL8 and OCI-LY19 showed no notable fraction of apoptotic cells. Two additional methods, TUNEL assay and DNA laddering as shown in Figure 2B-C, further confirmed the LY294002-induced apoptosis in LY-sensitive cells. SUDHL8 and OCI-LY19 were again found to be resistant to LY294002-induced apoptosis. These data indicate that inhibition of PI3K resulted in induction of apoptosis in majority of DLBCL cells. To further validate these findings, we used another PI3K inhibitor, wortmannin, and a direct AKT inhibitor to evaluate the sensitivity of these compounds on DLBCL cell lines. SUDHL4 and SUDHL8 cell lines were treated with 50 and 100 nM wortmannin and 20 and 40 μM AKT inhibitor for 24 hours. Trypan blue exclusion assay and annexin V/PI staining methods were used to evaluate cell death and apoptosis, respectively. Our data showed that wortmannin and AKT inhibitor induced apoptosis in SUDHL4, whereas no effect was seen in SUDHL8 cell line (Figure S2).

Constitutive activation of PKB/AKT signaling pathways in DLBCL cells

Activation of the PI3K has been studied in growth factor–independent cell lines through the phosphorylation of its downstream target, the serine-threonine kinase AKT (Ser473). By using antibody that recognizes activated AKT at Ser473, we sought to

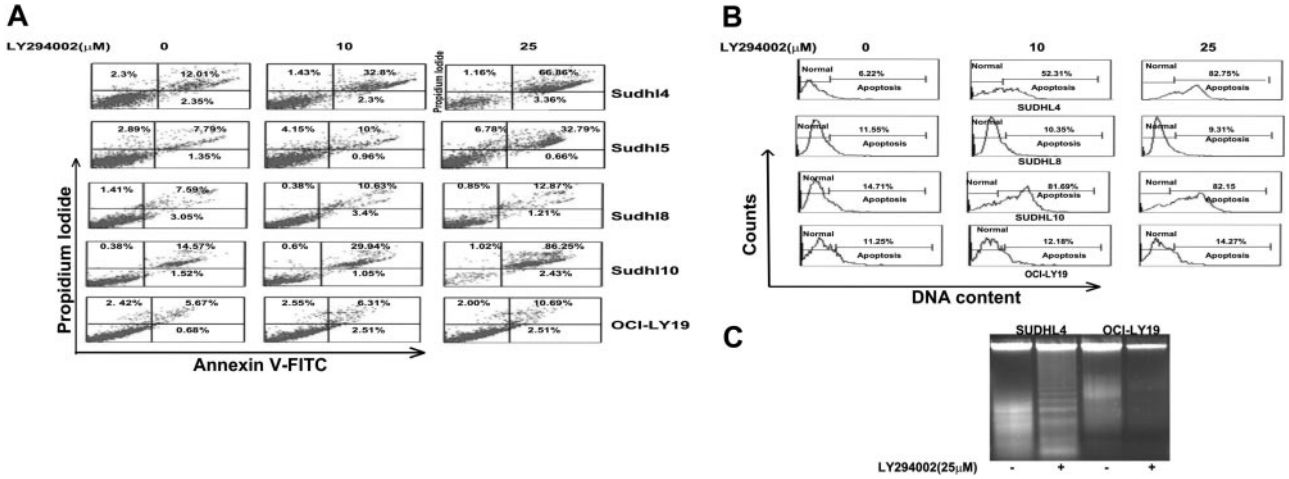

Figure 2. LY294002-induced apoptosis in DLBCL cell lines. (A) SUDHL-4, SUDHL-5, SUDHL-8, SUDHL-10, and OCI-LY19 cell lines were treated with 10 and 25 μM LY294002 for 24 hours and cells were subsequently stained with fluorescein-conjugated annexin V antibody and propidium iodide (PI) and the ratio of apoptotic cells was analyzed by flow cytometry. (B) SUDHL-4, SUDHL-8, SUDHL-10, and OCI-LY19 cells were treated with various doses of LY294002 for 24 hours and apoptosis was determined using TUNEL assays. (C) SUDHL-4 and OCI-LY19 cells were treated with 25 μM LY294002 for 24 hours and DNA was extracted and separated by electrophoresis on 1.5% agarose gel.

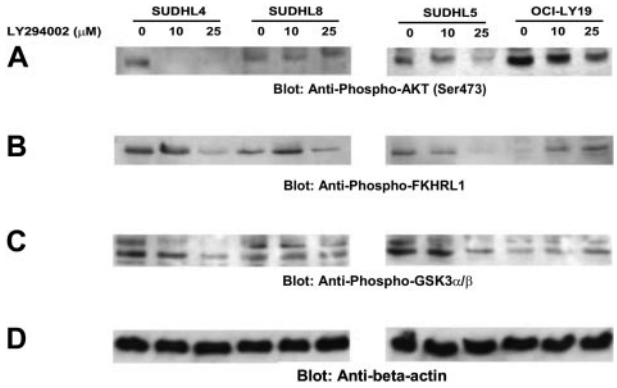

Figure 3. Inhibition of PI3K/AKT signaling pathway during LY294002-induced apoptosis. SUDHL-4, SUDHL-5, SUDHL8, and OCI-LY19 cells were treated with and without 10 and 25 μM LY294002 for 24 hours. After cell lysis equal amounts of proteins were separated by SDS-PAGE, transferred to Immobilon membrane, and immunoblotted with antibodies against phospho-AKT (Ser473), phospho FKHR, and phosphoGSK3α/β-actin as indicated.

determine the constitutive activation status of AKT in DLBCL cell lines as well as to determine whether inhibition of PI3K by LY294002 abrogates phosphorylation of AKT. DLBCL cell lines were treated in the presence and absence of LY294002 for 24 hours as indicated, cells were lysed, and proteins were analyzed by Western blot. As shown in Figure 3A, AKT was constitutively phosphorylated in the LY-sensitive as well as in the LY-resistant cell lines. Treatment with LY294002 dephosphorylated AKT in SUDHL4 and SUDHL5 cells, whereas LY294002 treatment did not produce any change in AKT phosphorylation level in SUDHL8 and OCI-LY19 cell lines.

The forkhead family of transcription factors has been reported as a downstream target of AKT, mediating apoptosis in other systems.[45] Active FKHR transcription factors promote transcription of genes involved in cell-cycle arrest and apoptosis.[46] One mechanism by which AKT promotes cell survival is by phosphorylating FKHR transcription factors, which inactivates them and prevents apoptosis.[47] We thus studied the level of FKHR/FOXO1 phosphorylation in LY294002-treated and -untreated DLBCL cells by Western blotting. As shown in Figure 3B, constitutive phosphorylation of FKHR was seen in all DLBCL cell lines, but LY294002 treatment resulted in dephosphorylation in LY-sensitive cell lines only and no effect was seen on the resistance of FKHRL phosphorylation in SUDHL8 and OCI-LY19 cell lines.

We next determined the activation of GSK3 in DLBCL cells, which has been recently reported to be a target of PI3K/AKT and is involved in promotion of cell survival.[48] All DLBCL cell lines showed constitutive phosphorylation of GSK3 and dephosphorylation in the presence of LY294002 (Figure 3C) was observed only in LY-sensitive cell lines with no significant effects in LY-resistant cells. These results suggest that AKT and its downstream effectors play a role in LY294002-induced apoptosis in DLBCL cell lines.

Effects of the inhibition of PI3K/AKT signaling at the mitochondrial level in DLBCL cells

The apoptotic signaling cascade starts with activation of caspase-8 and truncation of BID that translocates to the mitochondrial membrane allowing activation of proapoptotic proteins and release of cytochrome *c*. Therefore, we sought to determine whether inhibition of PI3K signaling involves the mitochondria. Activated caspase-8 is capable of cleaving caspase-3 either directly or by digesting BID to its active form (tBID), which leads to the release of cytochrome *c* from mitochondria.[49] LY294002 treatment for 24 hours resulted in activation of caspase-8 leading to truncation of BID in SUDHL4 and SUDHL5 cells (Figure 4A) as inferred by the decreased intensity of the full-length BID band. On the other hand, SUDHL8 and OCI-LY19 cell lines were resistant to LY294002-induced activation of BID and caspase-8. We then tested the effect of LY294002 on the mitochondrial membrane potentials in these cells. DLBCL cells were treated with 25 μM LY294002 for 24 hours and labeled with JC-1 dye and mitochondrial membrane potential was measured by flow cytometry. As shown in Figure 4B, inhibition of PI3K resulted in loss of mitochondrial membrane potential in SUDHL4, SUDHL5, and SUDHL10 cells as measured by JC-1–stained green fluorescence depicting apoptotic cells. In SUDHL8 and OCI-LY19 cells, no change in mitochondrial membrane was observed. We then studied release of cytochrome *c* from the mitochondria in cells treated for 24 hours with LY294002. Cytosolic-specific, mitochondria-free as well as mitochondrial extracts were prepared as described in "Patients, materials, and methods." Cytochrome *c* was released to the cytosol after LY294002 treatment in SUDHL4 and SUDHL5 but not in OCI-LY19 cells (Figure 4C). On the other hand, the level of cytochrome *c* decreased in the mitochondrial fraction of LY-sensitive cells only. These results suggest that inhibition of PI3K/AKT pathways disrupts the mitochondrial membrane potential leading to the release of cytochrome *c* to the cytosol. We then sought to determine whether LY294002-induced release of cytochrome *c* was capable of activation of caspase-3 and PARP. Figure 5A shows that LY294002 treatment resulted in the activation of caspase-3 and cleavage of PARP in SUDHL4 and SUDHL5 cells but not in

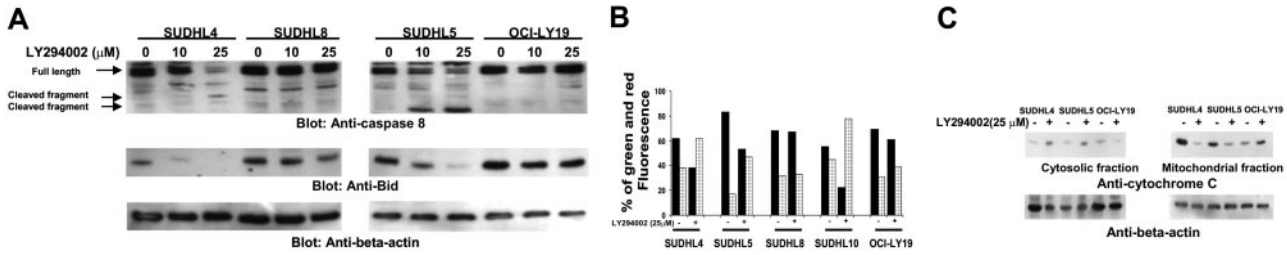

Figure 4. LY294002-induced activation of the mitochondrial apoptotic pathway in DLBCL cell lines. (A) LY294002-induced activation of caspase-8 and cleavage of BID. SUDHL-4, SUDHL-5, SUDHL-8, and OCI-LY19 cells were treated with 10 and 25 μM LY294002 for 24 hours. Cells were lysed and equal amounts of proteins were separated by SDS-PAGE, transferred to Immobilon membrane, and immunoblotted with antibodies against caspase-8, BID, and actin as indicated. (B) Loss of mitochondrial membrane potential by LY294002 treatment in DLBCL cells. SUDHL-4, SUDHL-5, SUDHL-8, SUDHL10, and OCI-LY19 cells were treated with and without 25 μM LY294002 for 24 hours. Live cells with intact mitochondrial membrane potential (■) and dead cells with lost mitochondrial membrane potential (▨) were measured by JC-1 staining and analyzed by flow cytometry as described in "Patients, materials, and methods." (C) LY294002-induced release of cytochrome *c*. SUDHL-4, SUDHL-5, and OCI-LY19 cell lines were treated with and without 25 μM LY294002 for 24 hours. Mitochondrial-free cytoplasmic as well as mitochondrial fractions were isolated as described in "Patients, materials, and methods." Cell extracts were separated on SDS-PAGE, transferred to PVDF membrane, and immunoblotted with antibodies against cytochrome *c* and actin as indicated.

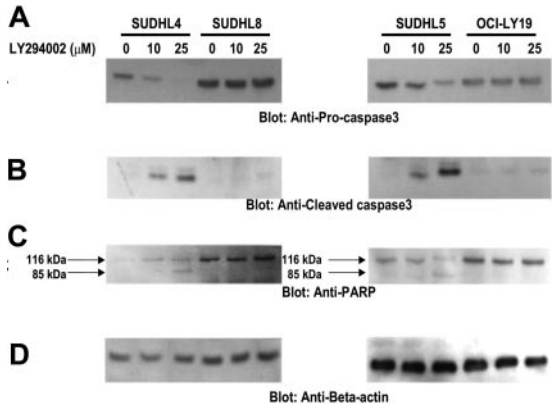

Figure 5. Activation of caspase-3 and cleavage of PARP induced by LY294002 treatment in DLBCL cells. SUDHL-4, SUDHL-5, SUDHL-8, and OCI-LY19 cells were treated with and without 10 and 25 μM LY294002 for 24 hours. Cells were lysed and equal amounts of proteins were separated by SDS-PAGE, transferred to PVDF membrane, and immunoblotted with antibodies against procaspase-3, cleaved caspase-3, PARP, and actin as indicated.

SUDHL8 and OCI-LY19 cells. These results are consistent with the data on cytochrome *c* release and indicate that activation of effector caspases participate in LY294002-induced apoptosis in DLBCL cells. In addition, pretreatment of DLBCL cells with 80 μM z-VAD-fmk, a universal inhibitor of caspases, abrogated apoptosis and prevented cell death and caspase-3 activation induced by LY294002 (Figure 6), clearly indicating that caspases play a critical role in LY294002-induced apoptosis in DLBCL cells. XIAP is a member of inhibitors of apoptosis protein family and a physiologic substrate of AKT that is stabilized to inhibit programmed cell death and has a direct effect on caspase-3 and caspase-9.[50] To determine whether XIAP plays a role in protecting DLBCL cells from LY294002-induced apoptosis, SUDHL4, SUDHL8, and SUDHL10 cells were treated with and without LY294002. Expression of XIAP

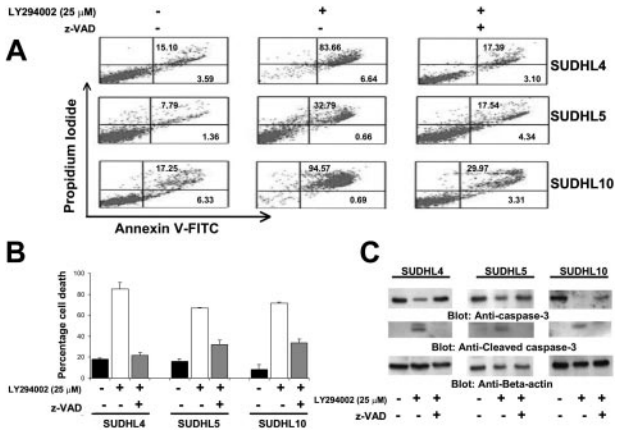

Figure 6. Effect of z-VAD on the LY294002-induced apoptosis. (A) Effect of z-VAD/fmk on LY294002-induced apoptosis in DLBCL cells. SUDHL-4, SUDHL-5, and SUDHL10 cells were pretreated with 80 μM z-VAD/fmk for 2 hours and subsequently treated with 10 and 25 μM LY294002 for 24 hours. Apoptosis was measured by annexin V/PI staining. (B) Effect of z-VAD/fmk on LY294002-induced cell death in DLBCL cells. SUDHL-4, SUDHL-5, and SUDHL-10 cells were pretreated with 80 μM z-VAD/fmk for 2 hours and subsequently treated with 10 and 25 μM LY294002 for 24 hours. Live and dead cells were scored using trypan blue exclusion dye. The graph displays the mean ± SD of 3 independent experiments. (C) z-VAD/fmk abrogates LY294002-induced activation of caspase-3. SUDHL-4, SUDHL-5, and SUDHL10 cells were pretreated with 80 μM z-VAD/fmk for 2 hours and subsequently treated with 25 μM for 24 hours. Cells were lysed and equal amounts of proteins were separated by SDS-PAGE, transferred to PVDF membrane, and immunoblotted with antibodies against procaspase-3, cleaved caspase, and actin as indicated.

was significantly decreased in sensitive SUDHL4 and SUDHL10 cells after LY294002 treatment, whereas no effect was seen in the resistant SUDHL8 cell line. These data suggest that XIAP is an important survival molecule that mediates AKT-induced cell survival in DLBCL cells (Figure S3).

Expression of activated AKT in DLBCL tumors

We subsequently stained DLBCL cell lines for p-AKT expression by immunohistochemistry (Figure 7). Our data showed that intensity of p-AKT staining was low in LY-sensitive cell lines (SUDHL 4, SUDHL10), whereas the expression was high in LY-resistant DLBCL cell lines (SUDHL8, OCI-LY19; Figure S4), suggesting that overexpression of p-AKT may be the cause of resistance to apoptosis. As a result of these findings, we sought to determine the expression pattern of p-AKT in patients with DLBCL. Using immunohistochemistry, p-AKT expression was high in 50 of 97 (51.54%) patients with interpretable data. We performed Kaplan-Meier survival analysis to determine the association of overall survival with p-AKT expression. Survival analysis was performed in 91 of the 97 p-AKT interpretable cases (6 patients had no follow-up data). A statistical trend toward inferior 5-year survival for patients with p-AKT$^+$ tumors was observed in the DLBCL (47 cases versus 44 cases, $P = .05$, not significant, log-rank).

Correlation of p-AKT with clinical and laboratory parameters

The major clinical and laboratory findings of the patients grouped according to high or low p-AKT expression are summarized in Table 1. All the parameters required to determine IPI were available in 64 patients; however, the LDH values were available in only 62 patients. Because these patients had a total IPI score of 4, they were categorized in the high-risk group and included in the analysis. In this patient population the IPI score correlated strongly with outcome ($P = .002$), consistent with previous studies.[37]

Although there were a higher proportion of patients with p-AKT overexpression in the high-risk group (high-intermediate risk and high-risk) as compared to the low-risk group (low-intermediate risk and low-risk), this was not statistically significant

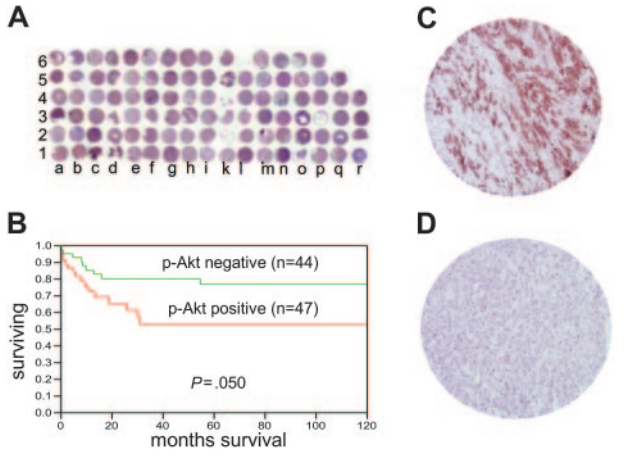

Figure 7. Tissue microarray-based p-AKT analysis in DLBCL patients. (A) Overview of the TMA containing 100 DLBCL tissue samples. (B) Kaplan-Meier survival curve of DLBCL of p-AKT expression by immunohistochemistry. (C) Immunohistochemistry of a tissue spot showing high p-AKT expression in DLBCL tumor (objective, 20×/0.70 NA). (D) A tissue spot showing negative p-AKT expression (objective, 20×/0.70 NA). Immunohistochemical staining images were obtained with a BX51 Olympus microscope and an Olympus DP12 camera (Olympus, Melville, NY). Images were viewed through a universal semi-apochromat objective lens (UPlan F1; Olympus America, Woodbury, NY). Magnifcation, 200×.

Table 1. Clinical characteristics and p-AKT Ser473 expression status of patients with DLBCL

		High p-AKT		Low p-AKT		
	Total	n	%	n	%	*P*
No. of patients	64	35	55	29	45	
Age, y						.279
60 or younger	35	17	49	18	51	
Older than 60	29	18	62	11	38	
Sex						.330
Female	17	11	65	6	35	
Male	47	24	51	23	49	
Performance status						.133
Lower than 2	40	19	48	21	52	
2 or higher	24	16	67	8	33	
Stage						.225
I or II	30	14	47	16	53	
III or IV	34	21	62	13	38	
Extranodal sites involved						.01
1 site	40	17	43	23	57	
More than 1 site	24	18	75	6	25	
LDH level*						.343
Normal	26	12	46	14	54	
High	36	21	58	15	42	
IPI						.111
Low to low-intermediate	35	16	46	19	54	
High-intermediate to high	29	19	66	10	34	
B symptoms						.003
Absent	29	10	35	19	65	
Present	35	25	71	10	29	
Ki-67 expression (n = 95)						.009
Positive	83	46	55	37	45	
Negative	12	2	17	10	83	

*LDH categorization is based on the range for normal values in the clinical laboratory at our institution. LDH levels were missing in 2 patients but both patients had a total IPI score of 4 and were categorized in the high-risk group.

($P = .114$). A more consistent correlative trend was noted in the proportion of p-AKT overexpressing tumors in the low-risk (39.1%), intermediate-risk (56%), and high-risk (75%) IPI groups ($P = .079$; Figure S5). Extranodal disease in more than one site was more common in patients with high p-AKT expression in the tumors than in patients with low p-AKT expression ($P = .01$). Presence of p-AKT overexpression was significantly associated ($P = .003$) with more frequent presentation in patients with B symptoms. In addition, Ki 67 expression, a proliferation marker, was significantly higher in p-AKT overexpressing DLBCL tumors ($P = .009$; Table 1).

Discussion

In the present study, we provide evidence that constitutive activation of the PI3K-PKB/AKT signaling pathway plays a critical role in regulating the growth and survival of DLBCL cells. Our data show that LY294002, a specific inhibitor of PI3K at 10 to 25 μM, causes apoptosis as determined by the increase of both sub-G_1 hypodiploid nuclei and annexin V^+ cell population. We also identified a set of DLBCL cell lines (SUDHL8 and OCI-LY19) that showed no response to LY294002-induced apoptosis (Figures 1-2). We found that PI3K is frequently activated, as confirmed by the detection of constitutive phosphorylation of different substrates downstream of PI3K, including AKT, FKHR, and GSK3 in all DLBCL cells tested (Figure 3). However, cell lines differed in the consequent effect on dephosphorylation of AKT, cytochrome *c* release from the mitochondria, and activation of caspase cascade system after LY294002 treatment. The oncogenic role of the deregulated PI3K pathway is probably related to its simultaneous actions on growth and survival. Different mechanisms of PI3K deregulation and activation have been reported in different systems. Amplification of the p110 subunit of PI3K is observed in ovarian cancer[51] and this catalytic subunit found in a chicken tumor virus mediates its transforming effects through AKT.[52] AKT is overexpressed in ovarian and pancreatic carcinomas.[53,54] A recent study has shown that growth factor deprivation induces proteolytic cleavage of the proapoptotic Bcl-2 family member BID to yield its active truncated form, tBID.[55] However, activated AKT inhibited mitochondrial cytochrome *c* release and apoptosis following BID cleavage. In concordance with this, our data show that inhibition of the PI3K/AKT pathway induced cleavage of BID, loss of mitochondrial membrane potential, and release of cytochrome *c* in those cells (SUDHL4 and SUDHL10) in which inhibition of PI3K dephosphorylated AKT. On the other hand, cell lines (SUDHL8 and OCI-LY19) that exhibit resistance to AKT, FKHR, and GSK3 dephosphorylation in response to LY294002 treatment did not lose mitochondrial potential and did not allow the release of cytochrome *c* to the cytosol. It has been shown that AKT inhibits apoptosis downstream of BID cleavage involving hexokinases.[55] AKT has also been shown to accumulate in the mitochondrial matrix and membrane after activation of PI3K.[56]

Apoptosis is a multistep process and an increasing number of genes have been identified that are involved in the control or execution of apoptosis.[57] Caspases play a crucial role in apoptosis. Among the 14 known members of IL-1–converting enzyme family of proteases, caspase-3 has been shown to be a key component of the apoptotic machinery.[58] Caspase-3 is activated in apoptotic cells and cleaves several cellular proteins, including PARP. The cleavage of PARP is used as a hallmark of apoptosis by various antitumor agents.[59] In this study, we show that inhibition of PI3K activates caspase-3 and cleaves PARP in LY294002-sensitive DLBCL cell lines. This implies that activation of caspase-3 is involved in LY294002-induced apoptosis.

The PI3K/AKT pathway is abnormally active in multiple tumor types, including lymphoid malignancies,[60,61] most frequently by inactivating mutations of PTEN but also by amplification and overexpression of PI3K/AKT.[62] Activated AKT has been shown to be associated with poor disease-free survival in patients with breast cancer and non–small-cell lung cancer.[63,64] The data from our DLBCL cell lines suggest that inhibition of PI3K by LY294002 induces an appreciable amount of apoptosis in cell lines with a low level of p-AKT expression as compared to cell lines that have relatively high expression of p-AKT. We have previously shown that inhibition of PI3K by LY294002 did not completely block the AKT phosphorylation in a primary effusion lymphoma cell line that caused resistance to LY294002-induced apoptosis.[33] The residual activated AKT protects the integrity of the mitochondrial membrane and does not allow the release of cytochrome *c*.[55] Furthermore XIAP, a physiologic substrate of AKT, is stabilized to inhibit programmed cell death and has a direct effect on caspase-3 and caspase-9.[50] Our data have shown that LY294002 treatment down-regulated XIAP in SUDHL4 and SUDHL10, whereas in SUDHL8 PI3K inhibition has no effect on the status of XIAP (Figure S3), suggesting phosphorylated AKT in SUDHL8 may protect XIAP from degradation in response to PI3K inhibition and render this cell line resistant to apoptosis. Our data suggest that in DLBCL cell lines where constitutive expression of AKT is either high or residual AKT activity remained after PI3K inhibition,

targeting of additional molecules such as XIAP in addition with PI3K inhibitor may overcome resistance and induce apoptosis.

Our immunohistochemistry data suggest that p-AKT overexpression in the DLBCL tissue array was associated with a poor outcome. Moreover, p-AKT overexpression was associated with a higher IPI score. In addition, it was significantly associated with involvement of more than one extranodal site and with B symptoms. A trend was seen with IPI score that did not reach statistical significance. Furthermore, high p-AKT expression was associated with relative risk of 1.4 for death in bivariate analysis in combination with IPI and 1.9 in univariate analysis by Cox regressional analysis (Table S1). However, bivariate analysis with IPI demonstrated no statistical significance ($P = .451$). This could be attributable to the small sample size, which was further reduced due to IPI being available only in 64 cases. These associations, we believe, would be significant if studied in a larger cohort of patients.

In summary, our results establish that the PI3K/AKT pathway is constitutively activated in human DLBCL cell lines. Inhibition of PI3K leads to apoptosis in most DLBCL cells through release of cytochrome *c* from the mitochondria and activation of downstream caspases. In addition, patients with high p-AKT expression showed a poor survival. These studies may have important implications for future preclinical and clinical studies in DLBCL. Not only could p-AKT expression be used for prognostication, but also, these findings may pave the way for investigations aimed at determining the usefulness of a novel strategy for treating DLBCL with inhibitors of the P13K/AKT pathway, either alone or in combination with other agents. Further animal, preclinical, and clinical studies are needed to validate the data presented here, which now have greater impact with recent identification of therapeutic strategies using inhibitors of small molecules.

Acknowledgment

We thank Dr Shakaib Siddiqui for collecting and reviewing clinical data.

Authorship

Contribution: S.U. designed research, performed experiments, analyzed data, and wrote the paper; A.R.H. designed research, performed experiments, analyzed data, and helped in writing the paper; A.K.S. analyzed data and did statistical analysis; P.S.M., N.A.A., A.M., and V.A. performed experiments; F.A., A.B., H.E., and A.E. provided clinical samples and data for performance of experiments and validation of data; P.B. performed experiments, analyzed data, did statistical analysis, and helped in writing the paper; and K.S.A. designed research, analyzed data, and helped in writing the paper.

Conflict-of-interest disclosure: The authors declare no competing financial interests.

Correspondence: Shahab Uddin, King Fahad National Center for Children's Cancer and Research, King Faisal Specialist Hospital and Research Center, MBC 98-16, PO Box 3354, Riyadh 11211, Saudi Arabia; e-mail: shahab@kfshrc.edu.sa.

References

1. The Non-Hodgkin's Lymphoma Classification Project. A clinical evaluation of the International Lymphoma Study Group classification of non-Hodgkin's lymphoma. Blood. 1997;89:3909-3916.
2. Muris JJ, Cillessen SA, Vos W, et al. Immunohistochemical profiling of caspase signaling pathways predicts clinical response to chemotherapy in primary nodal diffuse large B-cell lymphomas. Blood. 2005;105:2916-2923.
3. Hartge P Wang SS, Overview of the etiology and epidemiology of lymphoma. In: Mauch PM, Armitage JO, Coiffier B, Dalla-Favera R, Harris NL, eds. Non-Hodgkin's Lymphomas. New York, NY: Lippincott, Williams and Wilkins; 2004:711-727.
4. Smith PG, Wang F, Wilkinson KN, et al. The phosphodiesterase PDE4B limits cAMP-associated PI3K/AKT-dependent apoptosis in diffuse large B-cell lymphoma. Blood. 2005;105:308-316.
5. Lam LT, Davis RE, Pierce J, et al. Small molecule inhibitors of IkappaB kinase are selectively toxic for subgroups of diffuse large B-cell lymphoma defined by gene expression profiling. Clin Cancer Res. 2005;11:28-40.
6. Houldsworth J, Olshen AB, Cattoretti G, et al. Relationship between REL amplification, REL function, and clinical and biologic features in diffuse large B-cell lymphomas. Blood. 2004;103:1862-1868.
7. Pandolfi PP. Breast cancer—loss of PTEN predicts resistance to treatment. N Engl J Med. 2004;35:2337-2338.
8. Saal LH, Holm K, Maurer M, et al. PIK3CA mutations correlate with hormone receptors, node metastasis, and ERBB2, and are mutually exclusive with PTEN loss in human breast carcinoma. Cancer Res. 2005;65:2554-2559.
9. Zhang P, Ostrander JH, Faivre EJ, Olsen A, Fitzsimmons D, Lange CA. Regulated association of protein kinase B/Akt with breast tumor kinase. J Biol Chem. 2005;280:1982-1991.
10. Alessi DR, Cohen P. Mechanism of activation and function of protein kinase B. Curr Opin Genet Dev. 1998;8:55-62.
11. Al-Sakkaf KA, Mooney LM, Dobson PR, Brown BL. Possible role for protein kinase B in the anti-apoptotic effect of prolactin in rat Nb2 lymphoma cells. J Endocrinol. 2000;167:85-92.
12. Blanc A, Pandey NR, Srivastava AK. Synchronous activation of ERK 1/2, p38mapk and PKB/Akt signaling by H_2O_2 in vascular smooth muscle cells: potential involvement in vascular disease. Int J Mol Med. 2003;11:229-234.
13. Eves EM, Xiong W, Bellacosa A, et al. Akt, a target of phosphatidylinositol 3-kinase, inhibits apoptosis in a differentiating neuronal cell line. Mol Cell Biol. 1998;18:2143-2152.
14. West KA, Castillo SS, Dennis PA. Activation of the PI3K/Akt pathway and chemotherapeutic resistance. Drug Resist Updates. 2002;5:234-248.
15. Franke TF, Hornik CP, Segev L, Shostak GA, Sugimoto C. PI3K/Akt and apoptosis: size matters. Oncogene. 2003;22:8983-8998.
16. Bacus SS, Altomare DA, Lyass L, et al. AKT2 is frequently upregulated in HER-2/neu-positive breast cancers and may contribute to tumor aggressiveness by enhancing cell survival. Oncogene. 2002;21:3532-3540.
17. Luo J, Manning BD, Cantley LC. Targeting the PI3K-Akt pathway in human cancer: rationale and promise. Cancer Cell. 2003;4:257-262.
18. Nicholson KM, Anderson NG. The protein kinase B/Akt signalling pathway in human malignancy. Cell Signal. 2002;14:381-395.
19. Testa JR, Bellacosa A. AKT plays a central role in tumorigenesis. Proc Natl Acad Sci U S A. 2001; 98:10983-10985.
20. Wendel HG, De Stanchina E, Fridman JS, et al. Survival signaling by Akt and eIF4E in oncogenesis and cancer therapy. Nature. 2004;428:332-337.
21. Johnstone RW, Ruefli AA, Lowe SW. Apoptosis: a link between cancer genetics and chemotherapy. Cell. 2002;108:153-164.
22. Schmitt CA, Lowe SW. Bcl-2 mediates chemoresistance in matched pairs of primary E (mu)-myc lymphomas in vivo. Blood Cells Mol Dis. 2001;27: 206-216.
23. Rathmell JC, Thompson CB. The central effectors of cell death in the immune system. Annu Rev Immunol. 1999;17:781-828.
24. Kroemer G, Reed JC. Mitochondrial control of cell death. Nat Med. 2000;6:513-519.
25. Korsmeyer SJ. BCL-2 gene family and the regulation of programmed cell death. Cancer Res. 1999;59:1693s-1700s.
26. Schimmer AD, Welsh K, Pinilla C, et al. Small-molecule antagonists of apoptosis suppressor XIAP exhibits broad antitumor activity. Cancer Cell. 2004;5:25-35.
27. Uddin S, Hussain A, Manogaran PS, et al. Curcumin suppresses growth and induces apoptosis in primary effusion lymphoma. Oncogene 2005; 24:7022-7030.
28. Uddin S. Hussain A, Al-Hussein K, Platanias LC, Bhatia KG. Inhibition of phosphatidylinositol 3′-kinase induces preferentially killing of PTEN-null T leukemias through AKT pathway. Biochem Biophys Res Commun. 2004;320:932-938.
29. Hussain A, Doucet JP, Gutierrez M, et al. Tumor necrosis factor-related apoptosis-inducing ligand (TRAIL) and Fas apoptosis in Burkitt's lymphomas with loss of multiple pro-apoptotic proteins. Haematologica. 2003;88:167-175.
30. Krishan A. Rapid flow cytofluorometric analysis of mammalian cell cycle by propidium iodide staining. J Cell Biol. 1975;66:188-193.
31. Uddin S, Ah-Kang J, Ulaszek J, Mahmud D,

Wickrema A. Differentiation stage-specific activation of p38 mitogen-activated protein kinase isoforms in primary human erythroid cells. Proc Natl Acad Sci U S A. 2004;101:147-152.

32. Uddin S, Fish EN, Sher D, et al. The IRS-pathway operates distinctively from the Stat-pathway in hematopoietic cells and transduces common and distinct signals during engagement of the insulin or interferon-alpha receptors. Blood 1997;90: 2574-2582.
33. Uddin S. Hussain A, Manogaran PS, et al. Inhibition of phosphatidylinositol 3′-kinase/AKT-signaling promotes apoptosis of primary effusion lymphoma cells. Clin Cancer Res. 2005;11:3102-3108.
34. Hussain A, Al-Rasheed, Manogaran PS, et al. Curcumin induced apoptosis in acute T cell leukemias. Apoptosis 2005;11:245-254.
35. Kononen J, Bubendorf L, Kallioniemi A, et al. Tissue microarrays for high-throughput molecular profiling of tumor specimens. Nat Med. 1998;4: 844-847.
36. Jaffe ES, Harris NL, Stein H, Vardiman JW. Pathology and genetics of tumors of hematopoietic and lymphoid tissues: World Health Organization Classification of Tumors. Lyon, France; IARC Press: 2001.
37. The International Non-Hodgkin's Lymphoma Prognostic Factors Project. A predictive model for aggressive non-Hodgkin's lymphoma. N Engl J Med. 1993;329:987-994.
38. David O, Jett J, LeBeau H, et al. Phospho-Akt overexpression in non–small cell lung cancer confers significant stage-independent survival disadvantage. Clin Cancer Res. 2004;10:6865-6871.
39. Bose S, Chandran S, Mirocha JM, Bose N. The Akt pathway in human breast cancer: a tissue-array-based analysis. Mod Pathol. 2006;19:238-245.
40. Tsao AS, McDonnell T, Lam S, et al. Increased phospho-AKT (Ser473) expression in bronchial dysplasia: implications for lung cancer prevention studies. Cancer Epidemiol Biomarkers Prev. 2003;12:660-664.
41. Franke TF, Kaplan DR, Cantle LC. PI3K: downstream AKT1 on blocks apoptosis. Cell. 1997;88: 435-437,
42. Vlahos CJ, Matter WF, Hui KY, Brown RF. A specific inhibitor of phosphatidylinositol 3-kinase, 2-(4-morpholinyl)-8-phenyl-4H-1-benzopyran-4-one (LY294002). J Biol Chem. 1994;269:5241-5248.
43. Vlahos CJ, Matter WF, Brown RF, et al. Investigation of neutrophil signal transduction using a specific inhibitor of phosphatidylinositol 3-kinase. J Immunol. 1995;154:2413-2422.
44. Zhang C, Hazarika P, Ni X, Weidner DA, Duvic M. Induction of apoptosis by bexarotene in cutaneous T-cell lymphoma cells: relevance to mechanism of therapeutic action. Clin Cancer Res. 2002;8:1234-1240.
45. Brunet A, Park J, Tran H, Hu LS, Hemmings BA, Greenberg ME. Protein kinase SGK mediates survival signals by phosphorylating the forkhead transcription factor FKHRL1 (FOXO3a). Mol Cell Biol. 2001;21:952-965.
46. Alvarez B, Martinez-A C, Burgering BM, Carrera AC. Forkhead transcription factors contribute to execution of the mitotic programme in mammals. Nature. 2001;413:744-747.
47. Ciechomska I, Pyrzynska B, Kazmierczak P, Kaminska B. Inhibition of Akt kinase signalling and activation of forkhead are indispensable for upregulation of FasL expression in apoptosis of glioma cells. Oncogene. 2003;23:7617-7627.
48. Cross DA, Alessi DR, Cohen P, Andjelkovich M, Hemmings BA. Inhibition of glycogen synthase kinase-3 by insulin mediated by protein kinase B. Nature. 1378:785-789.
49. Gross A, McDonnell JM, Korsmeyer SJ. BCL-2 family members and the mitochondria in apoptosis. Genes Dev. 1999;13:1899-1911.
50. Dan HC, Sun M, Kaneko S, et al. Akt phosphorylation and stabilization of X-linked inhibitor of apoptosis protein (XIAP). J Biol Chem. 2004;279: 5405-5412.
51. Shayesteh L, Lu Y, Kuo WL, et al. PIK3CA is implicated as an oncogene in ovarian cancer. Nat Genet. 1999;21:99-102.
52. Chang HW, Aoki M, Fruman D, et al. Transformation of chicken cells by the gene encoding the catalytic subunit of PI 3-kinase. Science 1997; 276:1848-1850.
53. Bellacosa A, de Feo D, Godwin AK, et al. Molecular alterations of the AKT2 oncogene in ovarian and breast carcinomas. Int J Cancer. 1995;64: 280-285.
54. Cheng JQ, Ruggeri B, Klein WM, et al. Amplification of AKT2 in human pancreatic cells and inhibition of AKT2 expression and tumorigenicity by antisense RNA. Proc Natl. Acad Sci U S A. 1996; 93:3636-3641.
55. Majewski N, Nogueira V, Robey RB, Hay N. Akt inhibits apoptosis downstream of BID cleavage via a glucose-dependent mechanism involving mitochondrial hexokinases. Mol Cell Biol. 2004; 24:730-740.
56. Bijur GN, Jope RS. Rapid accumulation of Akt in mitochondria following phosphatidylinositol 3-kinase activation. J Neurochem. 2003;87:1427-1435.
57. Gastman BR. Apoptosis and its clinical impact. Head Neck. 2001;23:409-425.
58. Nunez G, Benedict MA, Hu Y, Inohara N. Caspases: the proteases of the apoptotic pathway. Oncogene. 1998;24:3237-3245.
59. Duriez PJ, Desnoyers S, Hoflack JC, et al. Characterization of anti-peptide antibodies directed towards the automodification domain and apoptotic fragment of poly (ADP-ribose) polymerase. Biochim Biophys Acta. 1997;1334:65-72.
60. Sakai A, Thieblemont C, Wellmann A, Jaffe ES, Raffeld M. PTEN gene alterations in lymphoid neoplasms. Blood. 1998;92:3410-3415.
61. Dahia PL, Aguiar RC, Alberta J, et al. PTEN is inversely correlated with the cell survival factor Akt/PKB and is inactivated via multiple mechanisms in haematological malignancies. Hum Mol Genet. 1999;8:185-193.
62. Vivanco I, Sawyers CL. The phosphatidylinositol 3-kinase AKT pathway in human cancer. Nat Rev Cancer. 2002;2:489-501.
63. Zhou X, Tan M, Stone Hawthorne V, et al. Activation of the Akt/mammalian target of rapamycin/4E-BP1 pathway by ErbB2 overexpression predicts tumor progression in breast cancers. Clin Cancer Res. 2004;10:6779-6788.
64. David O, Jett J, LeBeau H, et al. Phospho-Akt overexpression in non-small cell lung cancer confers significant stage-independent survival disadvantage. Clin Cancer Res. 2004;10:6865-6871.